Disparate requirements for the Walker A and B ATPase motifs of human RAD51D in homologous recombination

Claudia Wiese[1*], John M. Hinz[2], Robert S. Tebbs[2], Peter B. Nham[2], Salustra S. Urbin[2], David W. Collins[1], Larry H. Thompson[2] and David Schild[1]

[1] Life Sciences Division, Lawrence Berkeley National Laboratory, Berkeley, CA 94720

[2] Biosciences Directorate, Lawrence Livermore National Laboratory, P.O. Box 808, Livermore, CA 94551

*To whom correspondence should be addressed. Tel: +1 510 486 4024; Fax: +1 510 486 6816; Email: cwiese@lbl.gov

ABSTRACT

In vertebrates, homologous recombinational repair (HRR) requires RAD51 and five RAD51 paralogs (XRCC2, XRCC3, RAD51B, RAD51C, and RAD51D) that all contain conserved Walker A and B ATPase motifs. In human RAD51D we examined the requirement for these motifs in interactions with XRCC2 and RAD51C, and for survival of cells in response to DNA interstrand crosslinks. Ectopic expression of wild type human RAD51D or mutants having a non-functional A or B motif was used to test for complementation of a *rad51d* knockout hamster CHO cell line. Although A-motif mutants complement very efficiently, B-motif mutants do not. Consistent with these results, experiments using the yeast two- and three-hybrid systems show that the interactions between RAD51D and its XRCC2 and RAD51C partners also require a functional RAD51D B motif, but not motif A. Similarly, hamster Xrcc2 is unable to bind to the non-complementing human RAD51D B-motif mutants in co-immunoprecipitation assays. We conclude that a functional Walker B motif, but not A motif, is necessary for RAD51D's interactions with other paralogs and for efficient HRR. We present a model in which ATPase sites are formed in a bipartite manner between RAD51D and other RAD51 paralogs.

INTRODUCTION

DNA double-strand breaks (DSBs) represent a severe form of DNA damage that can lead to mutations and cell death if repaired incorrectly. Cells have evolved multiple mechanisms to repair DSBs, including the high fidelity process of homologous recombinational repair (HRR) (1,2), which contributes significantly to the repair of DSBs in cycling cells (3), such as those generated at the replication fork during interstrand crosslink (ICL) removal. In vertebrates, HRR is highly conserved and mediated by the bacterial RecA ortholog, the Rad51 recombinase, and five Rad51 paralogs (XRCC2, XRCC3, Rad51B, Rad51C and Rad51D). Though the biochemical functions of these paralogs in HRR are not well understood, they have been proposed to function in early steps (4-7) and in late steps (7-11) of recombination. The Rad51 paralogs are necessary for cellular resistance to DSBs (12,13), have no functional redundancy (14) and share limited sequence homology with Rad51 and with each other (~20% identity; reviewed in (15)). The regions of highest sequence homology are the putative ATP-binding domains: the conserved Walker A and Walker B motifs (12,13,15,16).

In human cells, several RAD51 paralog complexes have been identified, among them the RAD51B-RAD51C-RAD51D-XRCC2 heterotetramer, and three heterodimers: RAD51B-RAD51C, RAD51D-XRCC2 and RAD51C-XRCC3 (4,17-24). The RAD51B-RAD51C and RAD51D-XRCC2 complexes were shown to bind to single- and double-stranded DNA and to hydrolyze ATP, an activity enhanced by DNA binding (4,19,25,26). The heterotetramer also exhibits ATPase activity and preferentially bound to Y-shaped DNA and synthetic Holliday junctions (27).

The Walker ATPase domain (28) consists of two separate motifs, A and B, crucial components of the nucleotide-binding site. The lysine residue in the GKT/S box of the Walker A motif is essential for ATP-binding and contacts the γ-phosphate of the nucleotide (29). The highly conserved aspartate/glutamate of the Walker B motif forms hydrogen bonds with the threonine/serine of the GKT/S box and with a bound water molecule (30) and facilitates nucleotide hydrolysis.

In human RAD51, non-conservative (no ATP binding) K133A substitution in the Walker A motif did not rescue the Rad51-deficient lethality of chicken DT40 cells while the conservative (ATP binding, but no hydrolysis) K133R substitution only gave a partially defective phenotype (31). In *in vitro* assays, human RAD51-K133R showed an increased stability of presynaptic filament formation and enhanced homologous pairing activity compared to the wild type protein (32), but in a dominant-negative approach, expression of human RAD51-K133R in a mouse embryonic stem cell line specifically inhibited homology-directed DSB repair (33). In the Walker B motif of human RAD51, mutation in the highly conserved aspartate (D222A), but not V221A or S223A, was shown to eliminate protein function in the DT40 system (31). For the human RAD51 paralogs, mutations within the Walker A motif of RAD51C and XRCC3 were shown to greatly reduce cellular resistance to interstrand crosslinks (ICLs) (34,35), but mutation in the Walker A motif in XRCC2 had little effect on complementing ability (36). Substitution of the conserved aspartate residue in the Walker B motif of human XRCC3 (D213N) resulted in increased spontaneous apoptosis and complete loss of gene-complementing activity for cell survival to ICL damage in the CHO *xrcc3* mutant (37,38). Evidence suggests that nucleotide binding and hydrolysis play important roles in the formation of RAD51 paralog complexes. For example, in XRCC3, the inability to hydrolyze bound ATP (i.e. a Walker A GRT substitution) blocks the interaction with RAD51C (35). A study of the paralog interactions of mouse Rad51D Walker A mutants has also been reported (39), and these results are discussed later.

In this study, Walker-motif mutants of RAD51D were tested for their ability to complement the MMC sensitivity of CHO *RAD51D* knockout cells ((hereafter written as *rad51d* cells); (2)). Surprisingly, RAD51D mutants of the GKT box of the Walker A motif rescued the MMC sensitivity of *rad51d* cells, whereas B-motif mutants did not complement. In addition, whereas A-motif mutations had little effect on the interaction of RAD51D with binding partners XRCC2 and RAD51C, mutations in the B-motif disrupted these interactions. These results constitute the novel finding of a *differential* requirement for the Walker A and B motifs of a human ATPase.

EXPERIMENTAL PROCEDURES

Cell culture

Parental CHO cells (strain AA8) and 51D1Lox and 51D1 (*rad51d*) derivatives (2) were grown in monolayer or suspension cultures in MEM-alpha medium supplemented with 10% fetal bovine serum, 100 μg/ml streptomycin and 100 U/ml penicillin. For the experiments involving chronic MMC exposures and the generation of denatured and crude protein lysates from *rad51d* derivatives, cells were grown under selection in 700 μg/ml hygromycin B.

Human RAD51D expression plasmids

The *RAD51D* cDNA was PCR amplified from plasmid pDS200 (40) and subcloned into pcDNA3.1/*hygro* (Invitrogen) from HindIII to NheI. The entire *RAD51D* open reading frame (ORF) was verified by direct sequencing. Mutations were introduced using the QuickChange Site-directed mutagenesis II kit (Stratagene), and missense mutations were confirmed by direct sequencing of the entire ORF. Mutagenic primers were designed to create the following changes to the amino acid sequence of RAD51D: K113R, 5'-GGCCCAGGTAGCGGCCGCACTCAGGTATGTCTCTGTATGGC-3'; K113A, 5'-GGCCCAGGTAGCGGCGCTACTCAGGTATGTCTCTGTATGGC-3'; V203E, 5'-GGAACTGTGAAGGTGGAGGTTGTGGACTCGGTCACTGCGG-3'; and D206A, 5'-GGAACTGTGAAGGTGGTGGTTGTGGCTTCGGTCACTGCGG-3' (only forward primers are shown; reverse primers had the complementary sequence).

Yeast two- and three-hybrid system

The yeast strain Y190-ura$^-$ (40) was used for all yeast two- and three-hybrid experiments. For yeast two-hybrid analyses, Y190-ura$^-$ was co-transformed with both a DNA-binding domain (pGBT9; (41)) and a transcription-activating domain fusion plasmid (pGAD424; (41)) and transformants were recovered on selective media (i.e. synthetic complete media lacking leucine and tryptophan: SC -Leu, -Trp). For yeast three-hybrid analyses, RAD51B was expressed from pVT100U, a yeast expression vector containing the *URA3* selectable marker (42) as described in (40). To test three-hybrid interactions, strains containing two plasmids, grown in SC -Leu, -Ura, were transformed with the third plasmid, derived from pGBT9, and selected on plates lacking leucine, tryptophan and uracil. Four independent colonies for all transformations were assayed qualitatively for β-galactosidase activity using X-gal filter assay (43). To quantify the strength of protein-protein interactions, liquid β-galactosidase assays were performed using *o*-nitrophenyl-β-galactopyranoside (Sigma) as a substrate as described (43). All quantitative β-galactosidase activity assays were performed on three to five independent colonies, each monitored in triplicate. Standard error of the mean (SEM) was determined among independent colonies. Yeast two-hybrid plasmids for *RAD51D*, *XRCC2* and *RAD51C* are described in (40). Mutations were introduced into the *RAD51D* using site-directed mutagenesis and mutagenic primers as described above. Mutations were introduced into the *XRCC2* ORF using the QuickChange Site-directed mutagenesis II kit (Stratagene). Missense mutations were confirmed by direct sequencing of the entire ORF. Mutagenic primers for *XRCC2* were designed as follows: K54R, 5'-GGCCCAGAAGGAACAGGACGCACAGAAATGC-3'; K54A, 5'-GGCCCAGAAGGAACAGGAGCTACAGAAATGC-3'; L148S, 5'-

GCCTTTTGATTTTGGCCAGCCTGTCAGCTTTTTACTGG-3'; D148A, 5'-GCCTTTTGATTTCAGATAGCCTGTCAGCTTTTTACTGG-3'; (only forward primers are shown; reverse primers had the complementary sequence).

Whole cell protein extracts from transformed yeast strain Y190U-ura$^-$

To monitor the expression levels of Gal4-RAD51D in Y190U-ura$^-$ transformants, whole cell protein extracts were generated according to published procedures (44). Western blot analysis was carried out as described elsewhere (22), and filters were probed with 1:2000 diluted primary anti-RAD51D (Novus Biologicals). The signal for actin (dilution 1:300; Santa Cruz Biotech.) was used as a loading control. Detection was carried out using horseradish peroxidase-conjugated goat anti-rabbit secondary antibody (Jackson ImmunoResearch; 0.4 mg/ml). Filters were incubated with Supersignal WestPico substrate kit (Pierce Chemical) followed by exposure to Hyperfilm ECL (Amersham Biosciences).

Expression and purification of recombinant RAD51D and XRCC2 by affinity chromatography

For recombinant expression of GST-XRCC2 and His_6-RAD51D, respective cDNAs were inserted into the baculovirus transfer vector pFASTBAC^{TM} DUAL (Invitrogen). The *GST* ORF flanked by a PreScission Protease cleavage site was inserted upstream and in frame with the *XRCC2* ORF. For PCR amplification of the *RAD51D* cDNA an N-terminal His_6-tag was built in the forward primer. Proteins were expressed in Sf9 insect cells and purified to 80% homogeneity. One L of insect cell culture was harvested at 72 h post-infection, and cells were pelleted at 1600 × g and resuspended in 20 ml of cell lysis buffer (20 mM Hepes pH 8.0, 100 mM NaCl, 10% glycerol, 0.5 mM phenylmethylsulfonylfluoride (PMSF), 5 μg/ml aprotinin and 5 μg/ml leupeptin). The cell suspension was incubated on ice for 20 min, sonicated, and clarified by ultracentrifugation at 110,000 × g for 20 min. The supernatant was applied to a 5-ml Glutathione Sepharose 4 FF column (Amersham Biosciences) equilibrated with 10 column volumes buffer A (1 × phosphate buffered saline, 10% glycerol). Bound GST-XRCC2:His_6-RAD51D complex was washed with 10 column volumes buffer A and eluted with buffer B (10 mM glutathione, 50 mM Tris-HCl pH 8.0, 10% glycerol). Peak fractions were pooled and dialyzed into PreScission Protease cleavage buffer (50 mM Tris-HCl pH 8.0, 150 mM NaCl, 1 mM EDTA, 10% glycerol, 1 mM DTT, 0.5 mM PMSF, 5 μg/ml aprotinin and 5 μg/ml leupeptin) for subsequent cleavage by PreScission Protease according to the manufacturer's description (Amersham Biosciences). Following cleavage, the protein was diluted 1:1 with 100% glycerol and stored at -80°C.

Transfection of *rad51d* cells

Transfectants of *rad51d* cells (2) that stably express wild type or mutant human RAD51D protein were created by electroporation (625 V/cm, 950 μF) using Gene Pulser II (Bio-Rad). 1×10^6 cells were electroporated in 400 μl cytomix buffer using 10 μg of linearized plasmid (45). Twenty-four hours post-transfection, cells were plated into 10-cm dishes at ~ 10^4 cells/dish in 20 ml of medium containing hygromycin B (700 μg/ml) and incubated for 12 days for colony formation. Ten colonies were isolated and expanded for each transfected plasmid and analyzed for expression of the transgene by Western blot analysis (22). Filters were probed with 1:2000 diluted primary anti-RAD51D (Novus Biologicals). The signal for the transcription factor QM (dilution 1:10,000; Santa Cruz Biotech.) was used as a loading control. Detection was carried out using horseradish peroxidase-conjugated goat anti-rabbit secondary antibody (Jackson ImmunoResearch; 0.4 mg/ml). Filters were incubated with Supersignal WestPico substrate kit (Pierce Chemical) followed by exposure to Hyperfilm ECL (Amersham Biosciences).

Genetic complementation analysis

MMC sensitivity was determined by colony formation assay in 10-cm dishes. Exposure to MMC (Sigma) was conducted in 10-ml suspension cultures. For each dose, 1×10^6 cells were exposed to MMC for 60 min at 37°C, centrifuged, and resuspended in fresh medium for plating. For each dose, 300 or more cells were plated in triplicate. After 12 days of growth, dishes were rinsed with saline, fixed with 95% ethanol and stained with Gram Crystal Violet. Colonies with > 50 cells were scored.

To test for complementation directly in transfected cell populations, transfections were carried out as described above. Twenty-four hours post-transfection, cells were trypsinized and re-seeded at 4×10^4 cells/well in 6-well plates in regular growth medium containing hygromycin B without MMC, or with MMC at various concentrations. Colonies were fixed and stained after 12 days of growth. The surviving fraction of colonies was calculated as the ratio of the number of colonies in selection in MMC and hygromycin B to the number of colonies in the presence of hygromycin B only. For comparison purposes, untransfected AA8 were plated at 200 cells/well in regular growth medium lacking hygromycin B, both with and without MMC. In addition, *rad51d* cells were transfected with the empty vector control (pcDNA3.1/*hygro*) and plated at 4×10^4 cells/well in regular growth medium containing hygromycin B without or with MMC. The transfection efficiencies for all plasmids used were determined in a separate experiment. Plasmids were electroporated as described above and cells were plated 24 hr post transfection in regular growth medium containing hygromycin B. The stable transfection efficiencies were found to be similar for all plasmids used and were $0.27 \pm 0.03\%$.

Immunoprecipitation

Immunoprecipitation was performed as previously described (22) using native cellular protein extracts from untransfected *rad51d* and AA8 cells and *rad51d* cells stably expressing either wild type or mutant RAD51D. Immunoprecipitation was carried out using MagnaBind goat anti-rabbit IgG magnetic beads (Pierce) and anti-RAD51D antibody (Novus Biologicals) or control antibody (rabbit IgG, Santa Cruz Biotech.). The polyclonal rabbit anti-human XRCC2 antibody for direct immunoprecipitation of hamster Xrcc2 was kindly provided by Dr. P. Sung. Western blots were probed with 1:2000 diluted primary anti-RAD51D and 1:1000 diluted primary anti-XRCC2 antibody (Santa Cruz Biotech.). Detection was carried out using horseradish peroxidase-conjugated goat anti-rabbit secondary antibody (see above) or bovine anti-goat secondary antibody (1:10,000; Santa Cruz Biotech.). Filters were incubated as described above for analysis of RAD51D-expressing *rad51d* cells. To visualize co-immunoprecipitated hamster Xrcc2, filters were incubated with ECL-Advance (Amersham Biosciences).

RESULTS

Complementation of *rad51d* cells by ectopic expression of wild type human RAD51D

Following transfection of *rad51d* cells (clone 51D1; (2)) with the wild type RAD51D expression construct, colonies were selected for hygromycin resistance. To test whether these clones stably expressed the human cDNA, we picked 10 independent colonies and expanded them to mass cultures for Western blot analysis. As shown in Fig.1A, seven of these clones stably expressed the transgene. Since the expression levels for RAD51D protein varied, one clone expressing a lower level of the protein (WT1;

WT for wild type) and one expressing a higher level (WT2) were selected to test whether ectopic expression of human RAD51D rescued the very high (~80-fold) MMC sensitivity of *rad51d* cells (2). Using the colony formation assay for cell survival, we found that both clones WT2 and WT1 were efficiently complemented; their MMC resistance was similar to that of the wild type AA8 cells (Fig. 2A and 2B, respectively). We also observed that the parent of 51D1, 51D1Lox, which contains functional *Rad51D* alleles prior to Cre-recombinase treatment (2), was slightly more sensitive to MMC (~2-fold; determined form D_{37} values) than AA8 cells or *rad51d* cells expressing wild type human RAD51D (Fig. 2A and 2B). We explain this observation in part by the fact that the endogenous hamster Rad51D protein level in AA8 cells (and possibly the human protein in clones WT1 and WT2) is higher than in 51D1Lox cells (2). However, due to interspecies variation in antibody recognition it is not possible for us to compare the protein levels in 51D1Lox cells (i.e. hamster Rad51D) to that in the transfectants (i.e. human RAD51D).

Complementation of *rad51d* cells by ectopic expression of RAD51D Walker A-motif ATPase mutants

We tested whether a conservative amino acid substitution (K113R; binds but does not hydrolyze ATP), or a non-conservative substitution (K113A; unable to bind ATP), in the GKT box of the Walker motif A influenced the ability of RAD51D to complement the *rad51d* mutant. We transfected *rad51d* cells with each mutant construct (*G**R**T* and *GA**T*; see Fig. 1E) and isolated 10 independent clones for each mutant. As shown in Fig. 1B and 1C by Western blot analysis, the protein expression levels of independent clones stably expressing either mutant of RAD51D varied. As with the cells expressing the wild type *RAD51D* construct, for each mutant we choose a low-expressing clone (GAT2 and GRT3 (GRT2 was added in follow-up experiments); see Fig. 1, panels C and B, respectively), and a high expressing clone (GRT6 and GAT4; see Fig. 1, panels B and C, respectively). We found that stable expression of either mutant protein largely complemented MMC sensitivity of *rad51d* cells (Fig. 2A and 2B). The degree of MMC resistance of the high-expressing lines (GRT6 and GAT4) was similar to that of AA8 cells and *rad51d* cells expressing wild type RAD51D (WT2) (Fig. 2A). For the low-expressing lines (GRT2, GRT3 and GAT2), complementation was less complete (~2- to 3-fold lower, as determined from the D_{37} values (Fig. 2B)). However, these lower expressing lines were clearly no more sensitive to MMC than parental 51D1Lox cells that express reduced levels of hamster Rad51D (Fig. 2B; (2)).

No complementation of *rad51d* cells by ectopic expression of RAD51D Walker B-motif ATPase mutants

Since we observed almost no abnormality in cellular phenotype for the Walker A-motif mutations, we hypothesized that the Walker B motif may predominately determine the function of RAD51D. To test this possibility, we mutated the highly conserved aspartate (D206) to alanine (D206A; see Fig. 1E). For comparison purposes, we also made the previously uncharacterized V203E substitution within motif B of RAD51D. This valine was chosen for mutagenesis as it is conserved among the human RAD51 paralogs RAD51B, RAD51C, RAD51D and XRCC3, and in mouse and hamster Rad51D. Both expression constructs (*V203E* and *D206A*) were separately transfected into *rad51d* cells, and cells were selected in the continuous presence of either hygromycin alone or hygromycin plus increasing concentrations of MMC. The extent of complementation for expression of *all RAD51D* constructs was assessed by comparing the number of colonies arising in hygromycin and MMC to the number of colonies arising in hygromycin alone. As shown in Fig. 2C, ectopic expression of either RAD51D-V203E or RAD51D-

D206A does not result in complementation of MMC sensitivity of *rad51d* cells measured by colony formation. Conversely, in this same method of analysis, expression of wild type RAD51D, or the Walker A box mutants RAD51D-K113R and RAD51D-K113A resulted in high MMC resistance (Fig. 2C) albeit expression of either K113R or K113A did not fully protect against killing. Whether these latter modest reductions are biochemically significant is unclear since the expression levels of the A-motif mutant proteins could be slightly lower than that of wild type. As with the A-motif mutants, both B-motif mutants are expressed stably in *rad51d* cells (Fig. 1D).

Inability of RAD51D Walker B mutants to interact with XRCC2 in the yeast two-hybrid system

As RAD51D B-motif mutants are unable to repair MMC-induced DNA damage, we investigated whether disruptions occur in the interactions between RAD51D and its known paralog partners. To do so, we employed the yeast two- and three-hybrid systems and tested whether mutant RAD51D would be able to interact with either XRCC2 or RAD51C. Each of the described forms of RAD51D (wild type, K113R, K113A, V203E and D206A) was generated by site-directed mutagenesis using previously described vectors carrying wild type *RAD51D* (40). First, each RAD51D protein was tested for binding to wild type XRCC2 in both orientations (Fig. 3A). The average strength of the RAD51D-K113R:XRCC2 interactions was 75% or 57% of the wild type RAD51D:XRCC2 interaction (dependent on the orientation of the Gal4-fusion), and the average strength of RAD51D-K113A:XRCC2 interactions was very close to wild type levels (100% and 90%, depending on the orientation tested; see Fig. 3A).

Strikingly, both B-motif mutants displayed greatly reduced interaction with XRCC2 in either fusion orientation (Fig. 3A). The average strength of the RAD51D-V203E:XRCC2 interactions was determined to be at 1% and 3% of the wild type interaction, and the average strength of the RAD51D-D206A:XRCC2 interactions was at 3% and 11% of the wild type interaction (depending on the orientation tested). To ensure that the RAD51D mutants are produced in amounts adequate to detect positive protein interactions in the yeast two-hybrid system, we tested the protein expression levels for Gal4-RAD51D and its mutant forms by immunoblotting of total protein extracts (Fig. 3C). As for the wild type, all mutant forms of the Gal-RAD51D fusions were produced at high levels in yeast. Although K113R, V203E, and D206A were repeatedly expressed at slightly lower levels than the wild type and K113A, the failure of XRCC2 to interact with V203E and D206A is not due to the unavailability of these mutant proteins in yeast. For example, even though K113R and V203E are expressed at similar levels, they differ greatly in their ability to interact with XRCC2 (see Fig. 3C).

Inability of RAD51D Walker B mutants to interact with RAD51C in the yeast three-hybrid system

The interaction between human RAD51D and RAD51C, when tested in the yeast *two*-hybrid system, is comparatively weak, making it difficult to quantitatively assess protein-protein interactions that potentially are reduced even further. However, co-expression of RAD51B, in a non-fused form, has been shown previously to greatly enhance the strength of the RAD51D:RAD51C interaction in a yeast three-hybrid system (40). Furthermore, *in vivo* a stable RAD51D-RAD51C heterodimer has not been discovered, whereas RAD51D and RAD51C were shown to be part of the heterotetramer that also contains RAD51B and XRCC2 (20-22,24). For these reasons, we used the yeast three-hybrid system to assess the ability of either wild type or mutant RAD51D to interact with RAD51C when RAD51B is co-expressed. We found that the average strength of interactions between Walker A K113R and RAD51C was reduced to 60% of the wild type level, and the average strength of interactions between Walker A K113A and RAD51C was at 67% of the wild type interaction (Fig. 3B). Notably, the interactions between

RAD51D Walker B mutants and RAD51C were virtually eliminated, not differing from the negative control (Fig. 3B).

No co-immunoprecipitation of RAD51D Walker B mutants with hamster Xrcc2

To investigate *in vivo* complex formation between wild type or mutant human RAD51D and hamster Xrcc2, we performed reciprocal co-immunoprecipitation in extracts from *rad51d* clones that stably express the ectopic proteins at similar levels. We found that hamster Xrcc2 is present specifically in anti-RAD51D immunoprecipitated complexes from clone WT2 (which overexpresses wild type RAD51D) and not immunoprecipitated using IgG control antibody (Fig. 4A). In addition, CHO cells appear to express two isoforms of Xrcc2 (as indicated by the double arrows in Fig. 4A-C) that both bind to RAD51D. The faster migrating isoform displays the same mobility as recombinant human XRCC2 (Fig. 4C), while the second isoform appears to be larger and migrates with a shift that corresponds to a 2-3 kD difference in molecular weight. It is likely, but not clear yet, that this larger form of hamster Xrcc2 may be a modified version of the protein. We also have observed both isoforms of Xrcc2 in V79 hamster cells but not in mouse mammary epithelial cells (data not shown). Importantly, Xrcc2 was present in anti-RAD51D immunoprecipitated complexes from *rad51d* cells overexpressing A-motif mutants (K113R and K113A), but absent in anti-RAD51D immunoprecipitated complexes from B-motif mutants (D206A and V203E; Fig. 4B). Although reproducibly at lower levels compared to the wild type expressing line (WT2; here: GKT), Xrcc2 was always present in anti-RAD51D immunoprecipitated complexes from clones GAT4 and GRT6, which overexpress Walker A K113A and K113R mutant protein, respectively. Anti-RAD51D immunoprecipitated complexes from parental AA8 and *rad51d* cells contained neither RAD51D nor Xrcc2, demonstrating the inability of the anti-RAD51D antibody to recognize the hamster Rad51D protein in AA8 cells and the absence of human RAD51D in *rad51d* cells.

In reciprocal experiments we analyzed anti-Xrcc2 immunoprecipitated complexes from all cell lines for the presence of RAD51D (Fig. 4C). We found that the amounts of endogenous Xrcc2 directly precipitated by anti-XRCC2 antibody varied greatly among all cell lines tested (even though their expression levels for ectopic RAD51D were comparable; see Fig. 1). Only small amounts of Xrcc2 were precipitated from extracts of *rad51d* cells and *rad51d* cells expressing Walker B-motif mutants D206A or V203E (Fig. 4C). Significantly larger amounts of Xrcc2 were precipitated from cells overexpressing wild type RAD51D, K113R or K113A, and from AA8 cells. (Note: For AA8 cells only 1/16 of the amount of the precipitated complex was loaded onto the gel, relative to all other cell lines). We reproducibly detected wild type RAD51D (here: GKT), K113R, and K113A in anti-Xrcc2 immunoprecipitated complexes (Fig. 4C, lower panel). Not surprisingly, only small amounts of Walker B mutant proteins were present in anti-Xrcc2 complexes from *rad51d* cells overexpressing either V203E or D206A (Fig. 4C). In sum, these results show that ectopically expressed wild type RAD51D, or RAD51D with mutations in the Walker A motif, formed a stable complex with hamster Xrcc2. Conversely, motif-B mutants, although expressed at similar levels, had reduced levels of hamster Xrcc2, probably due to the inability to stabilize this protein as a RAD51D-Xrcc2 heterodimer (Fig. 5C; see Discussion).

Greatly impaired interaction of XRCC2-K54A and RAD51D in the yeast two-hybrid system

As we observed little decrease in interaction between RAD51D A-motif mutants and Xrcc2/XRCC2 both *in vivo* and in the yeast two-hybrid system, we hypothesized that XRCC2's Walker A motif participates in nucleotide-binding within the XRCC2-RAD51D heterodimer. Interestingly, a newly identified Rad51 paralog in *S. pombe*, Rlp1, having homology to human XRCC2 shows a conserved Walker A motif but no clearly defined Walker B motif (46). Therefore, we made the conservative K54R and non-conservative K54A substitutions in the Walker A motif of XRCC2, using previously described yeast two-hybrid plasmids (40), and assayed their interaction with wild type RAD51D, RAD51D-K113R or RAD51D-K113A qualitatively and in both orientations by X-Gal filter assay (Fig. 5A and 5B, respectively).

XRCC2-K54A was greatly impaired in binding to wild type RAD51D and mutant RAD51D (Fig. 5A and 5B, respectively; light blue and white colonies). However, XRCC2-K54R was able to interact with wild type RAD51D and both motif-A mutants of RAD51D (Fig. 5A and 5B, respectively). In addition, we introduced L148S or D149A amino acid substitutions within the Walker B motif of XRCC2 and assessed whether these XRCC2 mutants could interact with wild type RAD51D in the yeast two-hybrid system. Both XRCC2-L148S and XRCC2-D149A were impaired in binding to wild type RAD51D, although B-motif mutants of XRCC2 appeared to be less detrimental to the XRCC2:RAD51D interaction than B-motif mutants of RAD51D (Fig. 5C; see Discussion).

DISCUSSION

To our knowledge we have described the first human ATPase with disparate requirements for two highly conserved Walker A/B motifs, both of which are generally crucial components of the nucleotide-binding site. Because of the complete loss of RAD51D function caused by amino acid substitution within its conserved B motif, the contrasting finding, of normal biological function for GKT substitutions within the A motif, was quite unexpected. Moreover, a recent study of mouse Rad51D using *rad51d* mouse cells, in which only A-motif mutants were examined, reached the opposite conclusion, "that conservation of Walker Motif A is required for a physiological role of RAD51D" (39). Relative to the wild type control, these authors reported ~90% decrease in cell survival after exposure to MMC for K113R and K113A mutants in bulk transfected cell populations. However, these investigators did not perform standard MMC dose-response measurements to calculate the dose-reduction factor of cell sensitivity associated with the mouse Rad51D mutant forms. Since we also observed a slightly increased sensitivity to MMC (calculated by dose-reduction factor) under some conditions for both acute and chronic exposures (Fig. 2B and Fig. 2C), the only discrepancy between our survival data and theirs is the *extent* of reduced complementation by the A-motif mutants.

In addition, Gruver *et al*. reported moderately impaired interactions of mouse Rad51D A-motif mutants with Xrcc2, but strongly impaired interactions with Rad51C in the yeast two-hybrid system. Although we also found greatly impaired interactions between the human RAD51D Walker A mutants and RAD51C in yeast two-hybrid experiments when monitored qualitatively (data not shown), in the yeast three-hybrid system we found that these interactions were only moderately affected when tested in the presence of RAD51B. As discussed in the Results above, we believe that the yeast three-hybrid system more closely reflects the *in vivo* interaction context.

Similar to our finding of gross defects associated with the B-motif D206A mutant of RAD51D, human XRCC3 substitution at the corresponding aspartate (D213N) dramatically reduced MMC resistance when expressed in hamster *xrcc3* irs1SF cells (37). As suggested by others (31,37), substitution of this highly conserved aspartate likely disrupts ATP binding and/or hydrolysis activity. Nonetheless, XRCC3 does behave differently from RAD51D in that both Walker motifs are critical for XRCC3's function (35,37).

We presented evidence that alterations in the Walker B motif of RAD51D (V203E or D206A substitutions) greatly impair RAD51D-XRCC2 complex formation. Co-immunoprecipitation clearly shows that, in the presence of these non-complementing RAD51D mutant proteins, there is much less hamster Xrcc2 protein than under conditions where complementing RAD51D (i.e. wild type or motif-A mutants) is available. It is important to note from these experiments that the *rad51d* knockout cell line itself (i.e. untransfected) also expresses greatly reduced levels of endogenous Xrcc2 protein when compared to its AA8 parent line, which expresses wild type hamster Rad51D (Fig. 4C). Our findings are consistent with several studies showing the stabilization of RAD51 paralogs by each other *in vivo* (7,22,47,48), but our data additionally demonstrate that the ability to interact directly is required for this stabilization. In addition, neither Walker B-motif mutant is able to interact with the RAD51B:RAD51C heterodimer in the yeast three-hybrid system.

The loss of RAD51D-XRCC2 and RAD51D-RAD51C interactions by disruption of nucleotide binding (V203E or D206A substitutions) raises the question of which biochemical defect (nucleotide binding or protein-protein interaction) is responsible for the cellular phenotype of high sensitivity to MMC. Our preferred view is that the role of the ATPase activity that is blocked by the V203E and D206A substitutions is to mediate a conformational change that promotes tight binding of RAD51D with XRCC2 and/or RAD51C. In this model ATPase site integrity and protein interaction are inseparable.

Reiterative changes in protein conformation are important for the assembly of multi-subunit protein complexes that function in DNA repair (for review see (49)). Rad51 family members induce these conformational changes, necessary to fulfill protein function, by binding and hydrolysis of ATP (for review see (30)). X-ray crystal structures (50-54) and electron microscopy reconstructions (53-55) of several Rad51 homologs have provided evidence that ATP-binding occurs at the subunit interface by contacting several highly conserved residues on neighboring subunits. We surmise that human RAD51D, through its Walker B motif, may rely on the A motif of another RAD51 paralog to form an active ATPase.

Overall, our results suggest that RAD51D must form a complex with XRCC2 and/or RAD51C to maintain cellular resistance to MMC. We showed that both interactions require a normal RAD51D Walker B motif, but not an intact A motif. We speculate that the binding of ATP to RAD51D occurs through its Walker B box as part of a bipartite nucleotide-binding site interacting with XRCC2 and/or RAD51C, as illustrated in Fig. 6. In Fig. 6A, the B motif of RAD51D interacts with the A motif of XRCC2. We showed that mutations in either of these motifs block the interaction; disruption of the XRCC2 A motif via K54A substitution (but not K54R substitution) greatly diminishes its binding to RAD51D in the yeast two-hybrid system (Fig. 5A and 5B). One published observation is inconsistent with the idea that the RAD51D-XRCC2 interaction is important for efficient DNA repair. In that study, the XRCC2 A-motif K45A mutant showed only modest decrements in MMC resistance in irs1 V79 cells transfected with mutant proteins (36) (although Western blotting of these transfectants was not used to standardize the expressed XRCC2 protein levels). Moreover, in our yeast two-hybrid studies amino acid substitutions within the Walker B motif of XRCC2, though clearly affecting the XRCC2:RAD51D interaction, appear to be less deleterious to XRCC2:RAD51D complex formation in comparison with the RAD51D B-motif mutants (Fig. 5C). Fig. 6B depicts an ATPase site composed of the B motif of RAD51D and the A motif of RAD51C. Similar to our results for the B motif of RAD51D, mutations in the A motif of RAD51C also cause 80-100% loss of DNA repair efficiency (34). Although RAD51D-RAD51C interactions were not examined in that study, we found a severe RAD51D:RAD51C interaction defect in the yeast three-hybrid system for the RAD51D B-motif mutants (Fig. 3).

In conclusion, we provide evidence that the Walker B motif of human RAD51D is critically important for complex formation with other RAD51 paralogs and for cellular resistance to ICLs. Since both Walker B-motif substitutions (V203E and D206A) yielded a similar phenotype, we propose that these substitutions not only abrogate ATP hydrolysis, but also simultaneously prevent one or more critical interaction(s) and conformational changes underlying RAD51D's participation in complexes, whose integrity is necessary for recombinational repair.

ACKNOWLEDGEMENTS

The authors are grateful to Drs. M.-S. Tsai and M. Berardini for baculovirus transfer vector construction and help with protein purification. This work was supported by NCI/NIH P01 grant CA92584 (D.S.) titled Structural Cell Biology of DNA Repair Machines and NASA grant NNJ05HI36I (C.W.). The portion of this work done at LLNL was performed under the auspices of the U.S. Department of Energy by the University of California, Lawrence Livermore National Laboratory under Contract No. W-7405-

Eng-48 where the DOE Low-Dose Program and NCI/NIH grants CA89405 and CA112566 funded this work.

REFERENCES

1. Helleday, T. (2003) Pathways for mitotic homologous recombination in mammalian cells. *Mutat Res*, **532,** 103-115.
2. Hinz, J.M., Tebbs, R.S., Wilson, P.F., Nham, P.B., Salazar, E.P., Nagasawa, H., Urbin, S.S., Bedford, J.S. and Thompson, L.H. (2006) Repression of mutagenesis by Rad51D-mediated homologous recombination. *Nucleic Acids Res*, **34,** 1358-1368.
3. Rothkamm, K., Kruger, I., Thompson, L.H. and Lobrich, M. (2003) Pathways of DNA double-strand break repair during the mammalian cell cycle. *Mol Cell Biol*, **23,** 5706-5715.
4. Sigurdsson, S., Van Komen, S., Bussen, W., Schild, D., Albala, J.S. and Sung, P. (2001) Mediator function of the human Rad51B-Rad51C complex in Rad51/RPA-catalyzed DNA strand exchange. *Genes Dev*, **15,** 3308-3318.
5. Forget, A.L., Bennett, B.T. and Knight, K.L. (2004) Xrcc3 is recruited to DNA double strand breaks early and independent of Rad51. *J Cell Biochem*, **93,** 429-436.
6. Hatanaka, A., Yamazoe, M., Sale, J.E., Takata, M., Yamamoto, K., Kitao, H., Sonoda, E., Kikuchi, K., Yonetani, Y. and Takeda, S. (2005) Similar effects of Brca2 truncation and Rad51 paralog deficiency on immunoglobulin V gene diversification in DT40 cells support an early role for Rad51 paralogs in homologous recombination. *Mol Cell Biol*, **25,** 1124-1134.
7. Rodrigue, A., Lafrance, M., Gauthier, M.C., McDonald, D., Hendzel, M., West, S.C., Jasin, M. and Masson, J.Y. (2006) Interplay between human DNA repair proteins at a unique double-strand break in vivo. *Embo J*, **25,** 222-231.
8. Liu, Y., Masson, J.Y., Shah, R., O'Regan, P. and West, S.C. (2004) RAD51C is required for Holliday junction processing in mammalian cells. *Science*, **303,** 243-246.
9. Braybrooke, J.P., Li, J.L., Wu, L., Caple, F., Benson, F.E. and Hickson, I.D. (2003) Functional interaction between the Bloom's syndrome helicase and the RAD51 paralog, RAD51L3 (RAD51D). *J Biol Chem*, **278,** 48357-48366.
10. Brenneman, M.A., Wagener, B.M., Miller, C.A., Allen, C. and Nickoloff, J.A. (2002) XRCC3 controls the fidelity of homologous recombination: roles for XRCC3 in late stages of recombination. *Mol Cell*, **10,** 387-395.
11. Yonetani, Y., Hochegger, H., Sonoda, E., Shinya, S., Yoshikawa, H., Takeda, S. and Yamazoe, M. (2005) Differential and collaborative actions of Rad51 paralog proteins in cellular response to DNA damage. *Nucleic Acids Res*, **33,** 4544-4552.
12. Thacker, J. (1999) A surfeit of RAD51-like genes? *Trends Genet*, **15,** 166-168.
13. Thompson, L.H. and Schild, D. (1999) The contribution of homologous recombination in preserving genome integrity in mammalian cells. *Biochimie*, **81,** 87-105.
14. Takata, M., Sasaki, M.S., Tachiiri, S., Fukushima, T., Sonoda, E., Schild, D., Thompson, L.H. and Takeda, S. (2001) Chromosome instability and defective recombinational repair in knockout mutants of the five Rad51 paralogs. *Mol Cell Biol*, **21,** 2858-2866.
15. Thacker, J. (2005) The RAD51 gene family, genetic instability and cancer. *Cancer Lett*, **219,** 125-135.
16. Thompson, L.H. and Schild, D. (2001) Homologous recombinational repair of DNA ensures mammalian chromosome stability. *Mutat Res*, **477,** 131-153.
17. Braybrooke, J.P., Spink, K.G., Thacker, J. and Hickson, I.D. (2000) The RAD51 family member, RAD51L3, is a DNA-stimulated ATPase that forms a complex with XRCC2. *J Biol Chem*, **275,** 29100-29106.

18. Kurumizaka, H., Ikawa, S., Nakada, M., Eda, K., Kagawa, W., Takata, M., Takeda, S., Yokoyama, S. and Shibata, T. (2001) Homologous-pairing activity of the human DNA-repair proteins Xrcc3.Rad51C. *Proc Natl Acad Sci U S A*, **98,** 5538-5543.
19. Kurumizaka, H., Ikawa, S., Nakada, M., Enomoto, R., Kagawa, W., Kinebuchi, T., Yamazoe, M., Yokoyama, S. and Shibata, T. (2002) Homologous pairing and ring and filament structure formation activities of the human Xrcc2*Rad51D complex. *J Biol Chem*, **277,** 14315-14320.
20. Liu, N., Schild, D., Thelen, M.P. and Thompson, L.H. (2002) Involvement of Rad51C in two distinct protein complexes of Rad51 paralogs in human cells. *Nucleic Acids Res*, **30,** 1009-1015.
21. Miller, K.A., Yoshikawa, D.M., McConnell, I.R., Clark, R., Schild, D. and Albala, J.S. (2002) RAD51C interacts with RAD51B and is central to a larger protein complex in vivo exclusive of RAD51. *J Biol Chem*, **277,** 8406-8411.
22. Wiese, C., Collins, D.W., Albala, J.S., Thompson, L.H., Kronenberg, A. and Schild, D. (2002) Interactions involving the Rad51 paralogs Rad51C and XRCC3 in human cells. *Nucleic Acids Res*, **30,** 1001-1008.
23. Masson, J.Y., Stasiak, A.Z., Stasiak, A., Benson, F.E. and West, S.C. (2001) Complex formation by the human RAD51C and XRCC3 recombination repair proteins. *Proc Natl Acad Sci U S A*, **98,** 8440-8446.
24. Masson, J.Y., Tarsounas, M.C., Stasiak, A.Z., Stasiak, A., Shah, R., McIlwraith, M.J., Benson, F.E. and West, S.C. (2001) Identification and purification of two distinct complexes containing the five RAD51 paralogs. *Genes Dev*, **15,** 3296-3307.
25. Lio, Y.C., Mazin, A.V., Kowalczykowski, S.C. and Chen, D.J. (2003) Complex formation by the human Rad51B and Rad51C DNA repair proteins and their activities in vitro. *J Biol Chem*, **278,** 2469-2478.
26. Shim, K.S., Schmutte, C., Tombline, G., Heinen, C.D. and Fishel, R. (2004) hXRCC2 enhances ADP/ATP processing and strand exchange by hRAD51. *J Biol Chem*, **279,** 30385-30394.
27. Yokoyama, H., Sarai, N., Kagawa, W., Enomoto, R., Shibata, T., Kurumizaka, H. and Yokoyama, S. (2004) Preferential binding to branched DNA strands and strand-annealing activity of the human Rad51B, Rad51C, Rad51D and Xrcc2 protein complex. *Nucleic Acids Res*, **32,** 2556-2565.
28. Walker, J.E., Saraste, M., Runswick, M.J. and Gay, N.J. (1982) Distantly related sequences in the alpha- and beta-subunits of ATP synthase, myosin, kinases and other ATP-requiring enzymes and a common nucleotide binding fold. *Embo J*, **1,** 945-951.
29. Story, R.M., Weber, I.T. and Steitz, T.A. (1992) The structure of the E. coli recA protein monomer and polymer. *Nature*, **355,** 318-325.
30. Bell, C.E. (2005) Structure and mechanism of Escherichia coli RecA ATPase. *Mol Microbiol*, **58,** 358-366.
31. Morrison, C., Shinohara, A., Sonoda, E., Yamaguchi-Iwai, Y., Takata, M., Weichselbaum, R.R. and Takeda, S. (1999) The essential functions of human Rad51 are independent of ATP hydrolysis. *Mol Cell Biol*, **19,** 6891-6897.
32. Chi, P., Van Komen, S., Sehorn, M.G., Sigurdsson, S. and Sung, P. (2006) Roles of ATP binding and ATP hydrolysis in human Rad51 recombinase function. *DNA Repair (Amst)*, **5,** 381-391.
33. Stark, J.M., Hu, P., Pierce, A.J., Moynahan, M.E., Ellis, N. and Jasin, M. (2002) ATP hydrolysis by mammalian RAD51 has a key role during homology-directed DNA repair. *J Biol Chem*, **277,** 20185-20194.
34. French, C.A., Tambini, C.E. and Thacker, J. (2003) Identification of functional domains in the RAD51L2 (RAD51C) protein and its requirement for gene conversion. *J Biol Chem*, **278,** 45445-45450.
35. Yamada, N.A., Hinz, J.M., Kopf, V.L., Segalle, K.D. and Thompson, L.H. (2004) XRCC3 ATPase activity is required for normal XRCC3-Rad51C complex dynamics and homologous recombination. *J Biol Chem*, **279,** 23250-23254.

36. O'Regan, P., Wilson, C., Townsend, S. and Thacker, J. (2001) XRCC2 is a nuclear RAD51-like protein required for damage-dependent RAD51 focus formation without the need for ATP binding. *J Biol Chem*, **276,** 22148-22153.
37. Rafii, S., Lindblom, A., Reed, M., Meuth, M. and Cox, A. (2003) A naturally occurring mutation in an ATP-binding domain of the recombination repair gene XRCC3 ablates its function without causing cancer susceptibility. *Hum Mol Genet*, **12,** 915-923.
38. Lindh, A.R., Rafii, S., Schultz, N., Cox, A. and Helleday, T. (2006) Mitotic defects in XRCC3 variants T241M and D213N and their relation to cancer susceptibility. *Hum Mol Genet*, **15,** 1217-1224.
39. Gruver, A.M., Miller, K.A., Rajesh, C., Smiraldo, P.G., Kaliyaperumal, S., Balder, R., Stiles, K.M., Albala, J.S. and Pittman, D.L. (2005) The ATPase motif in RAD51D is required for resistance to DNA interstrand crosslinking agents and interaction with RAD51C. *Mutagenesis*.
40. Schild, D., Lio, Y.C., Collins, D.W., Tsomondo, T. and Chen, D.J. (2000) Evidence for simultaneous protein interactions between human Rad51 paralogs. *J Biol Chem*, **275,** 16443-16449.
41. Fields, S. (1993) The Two-Hybrid System to Detect Protein-Protein Interactions. *Methods*, **5,** 116-124.
42. Vernet, T., Dignard, D. and Thomas, D.Y. (1987) A family of yeast expression vectors containing the phage f1 intergenic region. *Gene*, **52,** 225-233.
43. Bartel, P.L. and Fields, S. (1995) Analyzing protein-protein interactions using two-hybrid system. *Methods Enzymol*, **254,** 241-263.
44. Hoffman, G.A., Garrison, T.R. and Dohlman, H.G. (2002) Analysis of RGS proteins in Saccharomyces cerevisiae. *Methods Enzymol*, **344,** 617-631.
45. van den Hoff, M.J., Moorman, A.F. and Lamers, W.H. (1992) Electroporation in 'intracellular' buffer increases cell survival. *Nucleic Acids Res*, **20,** 2902.
46. Khasanov, F.K., Salakhova, A.F., Chepurnaja, O.V., Korolev, V.G. and Bashkirov, V.I. (2004) Identification and characterization of the rlp1+, the novel Rad51 paralog in the fission yeast Schizosaccharomyces pombe. *DNA Repair (Amst)*, **3,** 1363-1374.
47. Lio, Y.C., Schild, D., Brenneman, M.A., Redpath, J.L. and Chen, D.J. (2004) Human Rad51C deficiency destabilizes XRCC3, impairs recombination, and radiosensitizes S/G2-phase cells. *J Biol Chem*, **279,** 42313-42320.
48. Xu, Z.Y., Loignon, M., Han, F.Y., Panasci, L. and Aloyz, R. (2005) Xrcc3 induces cisplatin resistance by stimulation of Rad51-related recombinational repair, S-phase checkpoint activation, and reduced apoptosis. *J Pharmacol Exp Ther*, **314,** 495-505.
49. Shin, D.S., Chahwan, C., Huffman, J.L. and Tainer, J.A. (2004) Structure and function of the double-strand break repair machinery. *DNA Repair (Amst)*, **3,** 863-873.
50. Wu, Y., He, Y., Moya, I.A., Qian, X. and Luo, Y. (2004) Crystal structure of archaeal recombinase RADA: a snapshot of its extended conformation. *Mol Cell*, **15,** 423-435.
51. Wu, Y., Qian, X., He, Y., Moya, I.A. and Luo, Y. (2005) Crystal structure of an ATPase-active form of Rad51 homolog from Methanococcus voltae. Insights into potassium dependence. *J Biol Chem*, **280,** 722-728.
52. Qian, X., Wu, Y., He, Y. and Luo, Y. (2005) Crystal Structure of Methanococcus voltae RadA in Complex with ADP: Hydrolysis-Induced Conformational Change. *Biochemistry*, **44,** 13753-13761.
53. Shin, D.S., Pellegrini, L., Daniels, D.S., Yelent, B., Craig, L., Bates, D., Yu, D.S., Shivji, M.K., Hitomi, C., Arvai, A.S. *et al.* (2003) Full-length archaeal Rad51 structure and mutants: mechanisms for RAD51 assembly and control by BRCA2. *Embo J*, **22,** 4566-4576.
54. Conway, A.B., Lynch, T.W., Zhang, Y., Fortin, G.S., Fung, C.W., Symington, L.S. and Rice, P.A. (2004) Crystal structure of a Rad51 filament. *Nat Struct Mol Biol*, **11,** 791-796.
55. VanLoock, M.S., Yu, X., Yang, S., Lai, A.L., Low, C., Campbell, M.J. and Egelman, E.H. (2003) ATP-mediated conformational changes in the RecA filament. *Structure (Camb)*, **11,** 187-196.

FIGURE LEGENDS

Figure 1. Representative Western blots showing the expression levels for wild type human RAD51D and its mutant forms in clonal isolates of stably transfected hamster *rad51d* cells. (**A**) *rad51d* clones expressing wild type human RAD51D, Upper panel: anti-RAD51D antibody; lower panel: anti-QM antibody (loading control). Extracts from untransfected *rad51d* cells is in left lanes of panels A-D. (**B**) *rad51d* clones expressing RAD51D-K113R (GRT1-GRT6) or RAD51D-K113A (GAT5 and GAT6); loaded for comparison; lower panel as in A. (**C**) *rad51d* clones expressing RAD51D-K113A (GAT2-GAT5) or wild type RAD51D (WT2; loaded for comparison purposes); lower panel as in A. (**D**) *rad51d* clones expressing RAD51D-D206A or RAD51D-V203E. Extract of clone WT2 (expressing wild type RAD51D) monitored for comparison purposes; lower panel as in A. The asterisk indicates that V203E runs with slightly slower mobility. "WB" indicates antibody used in Western blot analysis. (**E**) Domain structure of the RAD51D protein illustrating the amino acid substitutions introduced into the *RAD51D* cDNA. A: Walker A motif; B: Walker B motif. Highly conserved residues are underlined in the wild type sequence. Amino acid substitutions introduced are bold italics. Numbers indicate residue location within the primary sequence of RAD51D.

Figure 2. Cell survival determined by colony formation assay after acute or chronic exposure to MMC. (**A**) Parental lines and high-expressing transfectants carrying Walker A-motif mutations were exposed to MMC for 60 min. AA8, solid squares; 51D1Lox (*Rad51d*+), open squares; 51D1 (*rad51d*) expressing wild type human RAD51D (WT2), half-filled squares; 51D1 expressing Walker A-motif mutant, clone GAT4, solid diamonds; 51D1 expressing Walker A-motif mutant, clone GRT6, solid circles. (**B**) Parental, mutant (clone: 51D1), and low-expressing transfectants carrying Walker A-motif mutations were exposed to MMC for 60 min. Mutant 51D1 (*rad51d*), open diamonds; 51D1 expressing Walker A-motif mutant, clone GAT2, solid diamonds; 51D1 expressing Walker A-motif mutant, clone GRT2, solid triangle; 51D1 expressing Walker A-motif mutant, clone GRT3, solid circle; for AA8, 51D1Lox, and 51D1 expressing wild type RAD51D (here clone WT1) symbols same as in panel A. Horizontal line indicates D_{37} survival. (**C**) Survival of colony-forming ability in response to continuous MMC exposure of *rad51d* cells and transfectants expressing either wild type RAD51D (WT; open squares), K113R (open triangles), K113A (open circles), V203E (open diamonds), D206A (closed triangles). AA8 cells (closed circles) and *rad51d* cells transfected with the empty vector (pcDNA3.1/*hygro*; black cross) are shown for comparison. Error bars that are visible are ± 1 standard deviation from 3 independent experiments.

Figure 3. Yeast two- and three-hybrid analyses of the interactions of wild type or mutant RAD51D with XRCC2 or the RAD51C:RAD51B heterodimer, respectively. (**A**) Quantitative assessment of the RAD51D:XRCC2 interaction: β-galactosidase units determined photospectrometrically by using *o*-nitrophenyl-β-galactopyranoside as a substrate (one unit corresponds to ΔOD_{420nm}/min/mg protein). (**B**) Quantitative assessment of the RAD51D:RAD51B:RAD51C interaction: β-galactosidase units determined as in **A**. Results in **A** and **B** are from three to five different colonies for every interaction, each assayed in triplicate. Error bars represent ± 1 standard error of the mean; error bars that are not visible are too small to display. DBD = DNA binding domain of Gal4; AD = transactivating domain of Gal4; NF = non-fused protein (here: RAD51B). (**C**) Western blot to monitor the expression of Gal4-RAD51D wild type and mutant forms in yeast Y190U-ura$^-$ transformants. Three colonies for each transformation were

tested, and a representative blot is shown. Upper panel, anti-RAD51D antibody; lower panel, anti-actin antibody loading control.

Figure 4. RAD51D wild type and motif-A mutants allow complex formation with hamster Xrcc2 *in vivo*. (**A**) Crude extract from clone WT2 (overexpressing wild type human Rad51D) immunoprecipitated with a polyclonal antibody against RAD51D. Precipitated RAD51D (upper panel) and co-precipitated Xrcc2 (lower panel) were detected by Western blot analysis on the same membrane. A mock immunoprecipitate by incubation of WT2 extracts with IgG control antibody is shown in the far left lane. For comparison purposes, whole cell extract from clone WT2 is shown in the far right lane. Note: Xrcc2 is present in two isoforms in CHO cells (strain AA8 and derivatives; see also panel C). "HC" indicates cross-reacting heavy chain signal. "IP" indicates antibody used for immunoprecipitation. "WB" indicates antibody used in Western blot. (**B**) Presence of Xrcc2 in anti-RAD51D immunoprecipitated complexes from clones WT2 (GKT), GRT6 (K113R), and GAT4 (K113A). Xrcc2 is not present in anti-RAD51D complexes from parental AA8 (lane 2) or *rad51d* cells (neither cell line expresses human RAD51D that is precipitated here). For comparison, crude extracts from human cells (HeLa; far left lane), WT2 cells (GKT; second lane from the right), and AA8 cells (far right lane) are shown. Upper and lower panels: Western blot probed with Rad51D and XRCC2 antibodies, respectively. (**C**) Endogenous hamster Xrcc2 is expressed at higher levels in cell lines expressing complementing RAD51D (GKT, K113R, K113A) that is able to interact with Xrcc2. Upper panel: Western blot probed with anti-XRCC2 antibody shows two Xrcc2 isoforms in Xrcc2 immunoprecipitated complexes from *rad51d*, K113R, K113A, D206A, V203E, and GKT cell lines. Precipitated Xrcc2 from AA8 cells is shown for comparison (far left lane; note that only 1/16 of the precipitated complex relative to all other cell lines was loaded in order to avoid a very strong signal for Xrcc2). Two different concentrations of recombinant human XRCC2/$(His)_6$-RAD51D complex isolated from insect cells (second and third lanes from the left) and crude extract from clone WT2 (GKT; far right lane) are included. Lower panel: same blot probed with RAD51D antibody to detect human RAD51D that co-immunoprecipitated with hamster Xrcc2. Note: recombinant human His_6-tagged RAD51D migrated more slowly than human RAD51D.

Figure 5. Yeast two-hybrid analysis of the interactions between Walker A/B mutants of XRCC2 and RAD51D. (**A**) Greatly impaired XRCC2-K54A interaction with wild type RAD51D. Qualitative assessment: expression of β-galactosidase by X-gal filter assay; blue patches indicate the expression of interacting proteins; one representative colony is shown. (**B**) Pair wise analyses of the interaction between Walker A mutants from both XRCC2 and RAD51D. Qualitative assessment: as in **A**. (**C**) Comparative analysis of the interaction between either XRCC2-L148S or XRCC2-D149A and RAD51D or between XRCC2 and RAD51D-D206A. Results are from three different colonies for every interaction, each assayed in triplicate. Error bars represent ± 1 standard error of the mean. DBD = DNA binding domain of Gal4; AD = transactivating domain of Gal4.

Figure 6. Possible configurations of RAD51D interactions involving bipartite Walker A and B nucleotide binding motifs. (**A**) The RAD51D-XRCC2 heterodimer requires both the B motif of RAD51D and the A motif of XRCC2. (**B**) The RAD51D-RAD51C heterodimer requires the B motif of RAD51D; a requirement for the A motif of RAD51C is predicted but not yet been tested. Neither heterodimer requires the A motif of RAD51D. The possible role of the B motif of RAD51C has not been tested.

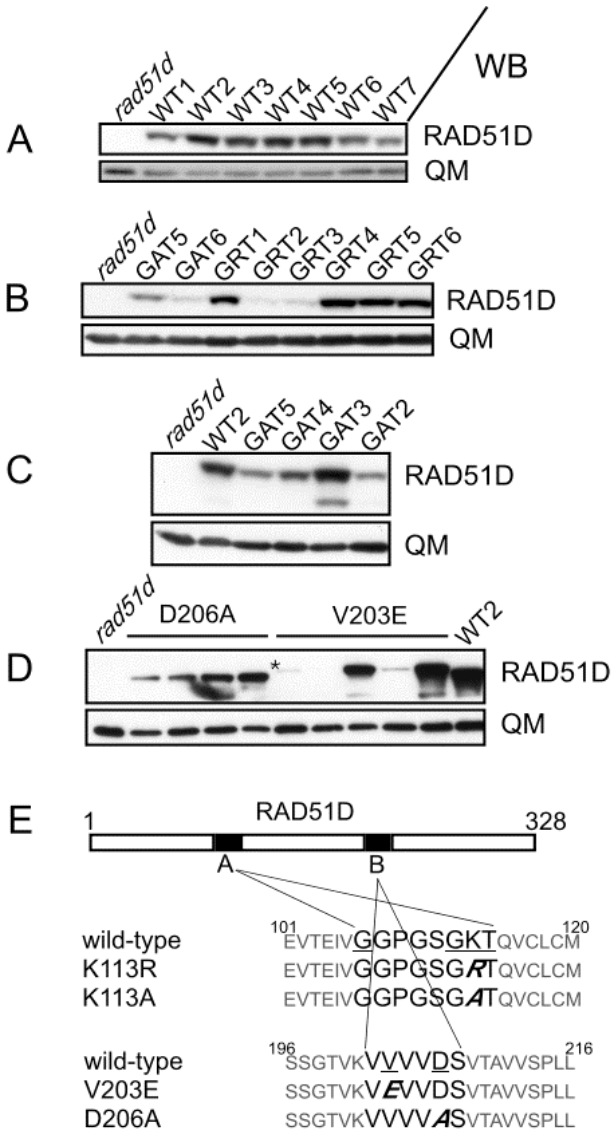
A
rad51d
WT1
WT2
WT3
WT4
WT5
WT6
WT7
WB
RAD51D
QM
B
rad51d
GAT5
GAT6
GRT1
GRT2
GRT3
GRT4
GRT5
GRT6
RAD51D
QM
C
rad51d
WT2
GAT5
GAT4
GAT3
GAT2
RAD51D
QM
D
rad51d
D206A
V203E
WT2
*
RAD51D
QM
E
1
RAD51D
328
A
B
wild-type 101 EVTEIVGGPGSGKT QVCLCM 120
K113R EVTEIVGGPGSGRT QVCLCM
K113A EVTEIVGGPGSGAT QVCLCM
wild-type 196 SSGTVKVVVVDS VTAVVSPLL 216
V203E SSGTVKVEVVDS VTAVVSPLL
D206A SSGTVKVVVVAS VTAVVSPLL

Figure 1

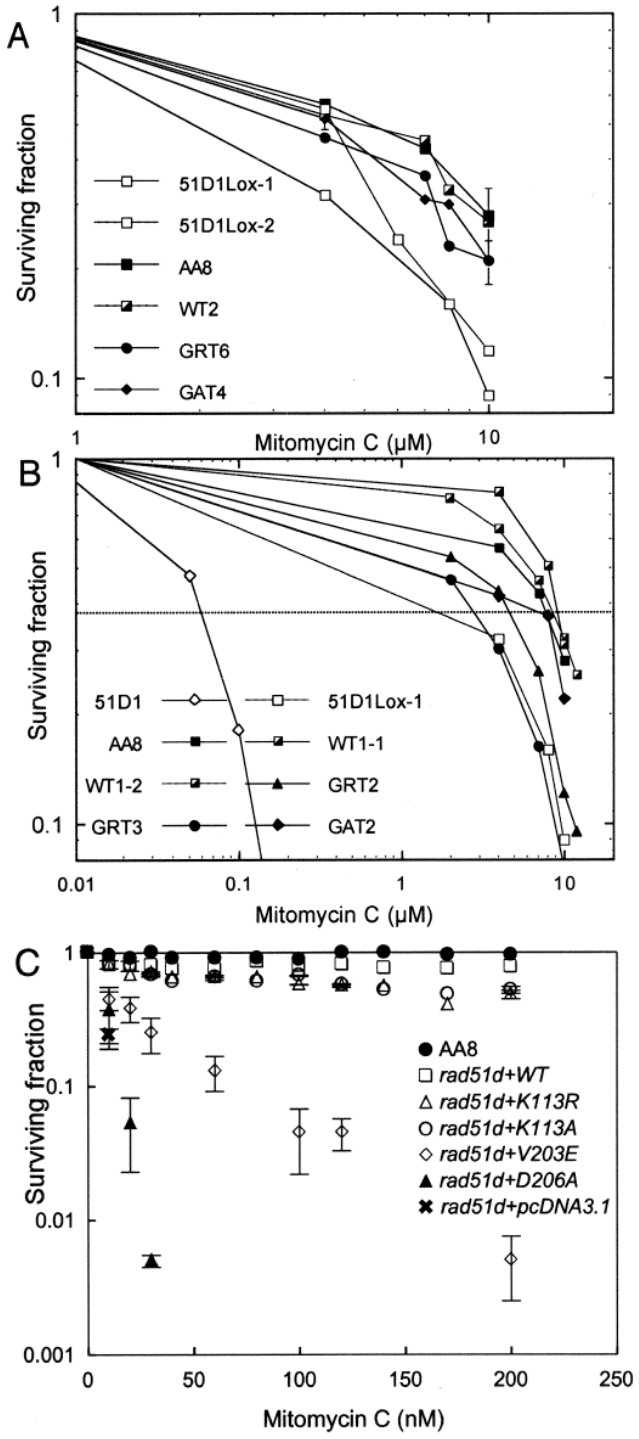
A
Surviving fraction
1
0.1
51D1Lox-1
51D1Lox-2
AA8
WT2
GRT6
GAT4
1
10
Mitomycin C (μM)
B
Surviving fraction
1
0.1
51D1
51D1Lox-1
AA8
WT1-1
WT1-2
GRT2
GRT3
GAT2
0.01
0.1
1
10
Mitomycin C (μM)
C
Surviving fraction
1
0.1
0.01
0.001
AA8
rad51d+WT
rad51d+K113R
rad51d+K113A
rad51d+V203E
rad51d+D206A
rad51d+pcDNA3.1
0
50
100
150
200
250
Mitomycin C (nM)

Figure 2

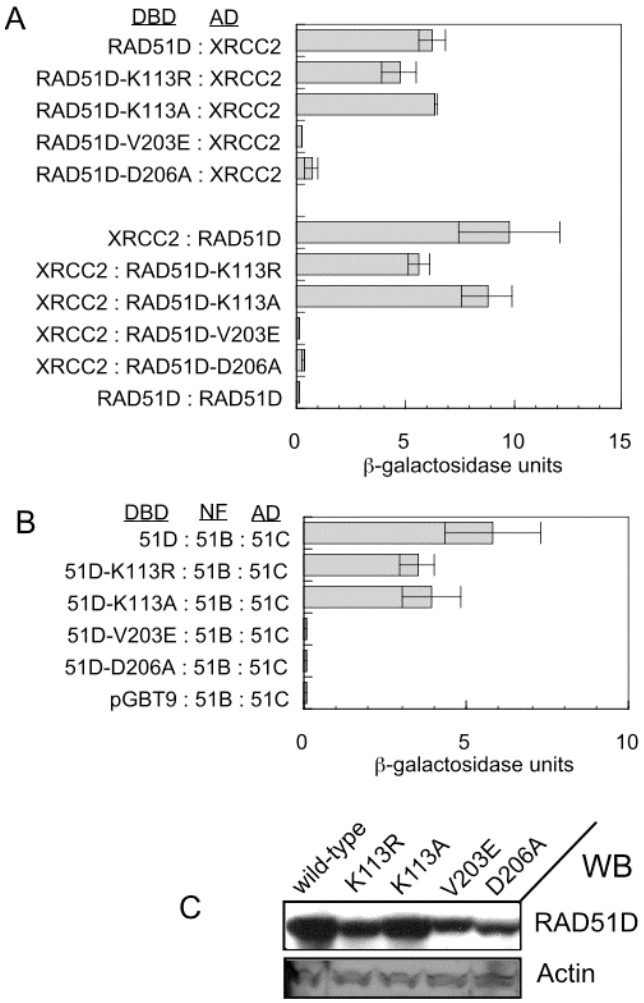
A
DBD AD
RAD51D : XRCC2
RAD51D-K113R : XRCC2
RAD51D-K113A : XRCC2
RAD51D-V203E : XRCC2
RAD51D-D206A : XRCC2
XRCC2 : RAD51D
XRCC2 : RAD51D-K113R
XRCC2 : RAD51D-K113A
XRCC2 : RAD51D-V203E
XRCC2 : RAD51D-D206A
RAD51D : RAD51D
0 5 10 15
β-galactosidase units
B
DBD NF AD
51D : 51B : 51C
51D-K113R : 51B : 51C
51D-K113A : 51B : 51C
51D-V203E : 51B : 51C
51D-D206A : 51B : 51C
pGBT9 : 51B : 51C
0 5 10
β-galactosidase units
C
wild-type
K113R
K113A
V203E
D206A
WB
RAD51D
Actin

Figure 3

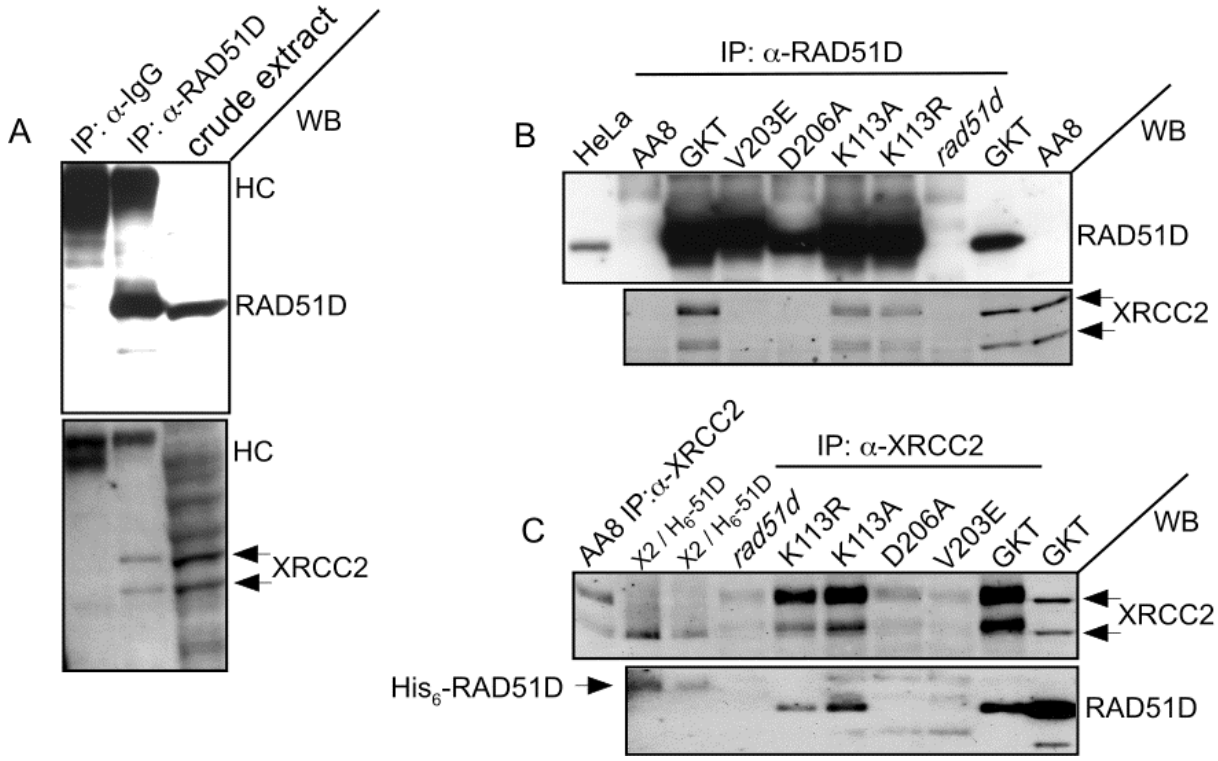
A
IP: α-IgG
IP: α-RAD51D
crude extract
WB
HC
RAD51D
HC
XRCC2
B
IP: α-RAD51D
HeLa
AA8
GKT
V203E
D206A
K113A
K113R
rad51d
GKT
AA8
WB
RAD51D
XRCC2
C
AA8 IP:α-XRCC2
X2 / H6-51D
X2 / H6-51D
IP: α-XRCC2
rad51d
K113R
K113A
D206A
V203E
GKT
GKT
WB
XRCC2
His6-RAD51D
RAD51D

Figure 4

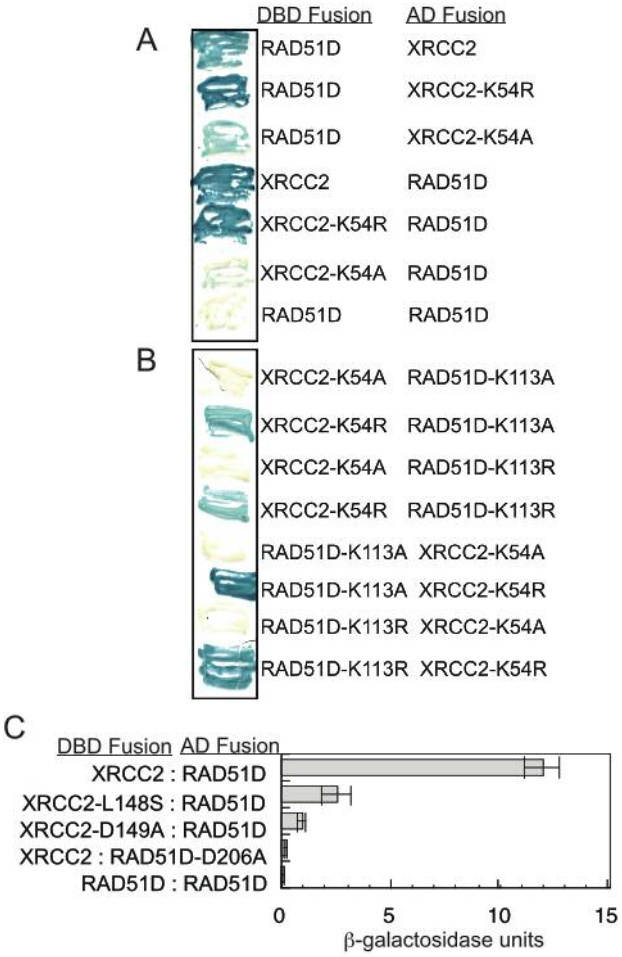
DBD Fusion
AD Fusion
A
RAD51D XRCC2
RAD51D XRCC2-K54R
RAD51D XRCC2-K54A
XRCC2 RAD51D
XRCC2-K54R RAD51D
XRCC2-K54A RAD51D
RAD51D RAD51D
B
XRCC2-K54A RAD51D-K113A
XRCC2-K54R RAD51D-K113A
XRCC2-K54A RAD51D-K113R
XRCC2-K54R RAD51D-K113R
RAD51D-K113A XRCC2-K54A
RAD51D-K113A XRCC2-K54R
RAD51D-K113R XRCC2-K54A
RAD51D-K113R XRCC2-K54R
C
DBD Fusion AD Fusion
XRCC2 : RAD51D
XRCC2-L148S : RAD51D
XRCC2-D149A : RAD51D
XRCC2 : RAD51D-D206A
RAD51D : RAD51D
0
5
10
15
β-galactosidase units

Figure 5

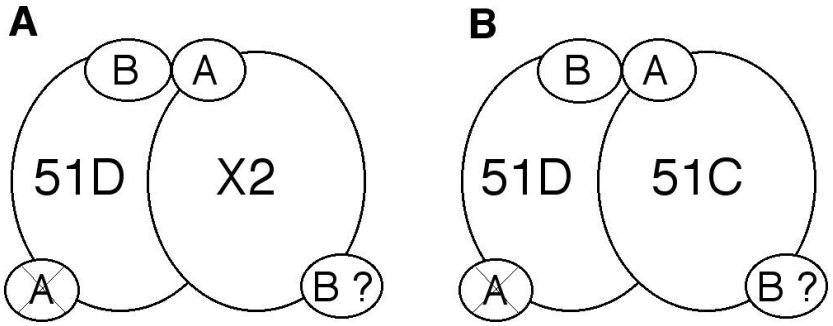

Figure 6